

OFDM-RSMA: Robust Transmission under Inter-Carrier Interference

Mehmet Mert Şahin, *Graduate Student Member IEEE*, Onur Dizdar, *Member, IEEE*, Bruno Clerckx, *Fellow, IEEE*, Huseyin Arslan, *Fellow, IEEE*

Abstract—Rate-splitting multiple access (RSMA) is a multiple access scheme to mitigate the effects of the multi-user interference (MUI) in multi-antenna systems. In this study, we leverage the interference management capabilities of RSMA to tackle the issue of inter-carrier interference (ICI) in orthogonal frequency division multiplexing (OFDM) waveform. We formulate a sum-rate maximization problem to find the optimal subcarrier and power allocation for downlink transmission in a two-user system using RSMA and OFDM. A weighted minimum mean-square error (WMMSE)-based algorithm is proposed to obtain a solution for the formulated non-convex problem. We show that the marriage of rate-splitting (RS) with OFDM provides complementary strengths to cope with peculiar characteristic of wireless medium and its performance-limiting challenges including inter-symbol interference (ISI), MUI, ICI, and inter-numerology interference (INI). The sum-rate performance of the proposed OFDM-RSMA scheme is numerically compared with that of conventional orthogonal frequency division multiple access (OFDMA) and OFDM-non-orthogonal multiple access (NOMA). It is shown that the proposed OFDM-RSMA outperforms OFDM-NOMA and OFDMA in diverse propagation channel conditions owing to its flexible structure and robust interference management capabilities.

Index Terms—Rate-splitting multiple access (RSMA), orthogonal frequency division multiplexing (OFDM), inter-carrier interference (ICI), multi-numerology OFDM

I. INTRODUCTION

Over the last two decades, the traffic in mobile broadband (MBB) networks has increased 50-70% each year all around the world [1]. Immense traffic growth results in the need for the capacity growth to maintain the quality of service. Compared to state-of-the-art wireless networks, next-generation wireless networks are expected to achieve significantly higher capacity, extremely low latency, ultra-high reliability, as well as massive and ubiquitous connectivity in order to meet diverse innovative applications, such as virtual reality (VR), augmented reality (AR), holographic communication, digital replica and non-terrestrial networks (NTN) networks [2]. Moreover, the evolution toward next-generation wireless networks requires a paradigm shift from

the communication-oriented design to a multi-functional design, including communication, sensing, imaging, computing, and highly accurate positioning capabilities with mobility. To meet these requirements of diverse applications, advanced multiple accessing schemes capable of supporting massive numbers of users are needed [3].

A. Background and Related Works

It has been shown that orthogonal transmission schemes are vulnerable to interference which destroy the orthogonality of the signalling scheme, such as, inter-symbol interference (ISI), inter-carrier interference (ICI), multi-user interference (MUI), adjacent channel interference (ACI), and inter-numerology interference (INI) [4]–[6]. Moreover, orthogonal transmission schemes can support a number of users limited by the given orthogonal resources [7]. Consequently, non-orthogonal transmission strategies have attracted interest from academia and industry for many years to meet the demand on explosively growing number of devices in next generation wireless networks (NGMA).

Since 2G mobile systems, different non-orthogonal transmission schemes are studied to circumvent the limitations encountered in the orthogonal transmission [8], [9]. Non-orthogonal spreading sequences are utilized in the form of IS-95, wideband code division multiple access (CDMA) (WCDMA), and CDMA2000, and serve as the core technologies of 2G and 3G. Moreover, multi-user superposition transmission (MUST) has been considered as a candidate multiple access scheme in 4G LTE-A, where messages of cell-edge and cell-interior users are proposed to be superimposed on the same resource element [10]. MUST scenario guarantees the decodability of messages exploiting substantial power difference between users. Another non-orthogonal transmission strategy that has gained popularity in recent years is called non-orthogonal multiple access (NOMA), which is studied in two forms, power-domain NOMA (PD-NOMA) and code-domain NOMA (CD-NOMA) [11]. PD-NOMA serves multiple users in the same time-frequency resource block, and separates them in the power domain using superposition coding (SC) and successive interference cancellation (SIC) techniques [12]. PD-NOMA allows superposition of users' messages for transmission, and the MUI ensuing from this non-orthogonal transmission is decoded and removed via SIC at the receiver. In single-antenna systems, e.g. single-input single-output (SISO) broadcast channels (BCs), PD-NOMA has been shown to achieve higher spectral efficiency (SE) than orthogonal multiple access (OMA) and simultaneously serve larger number of users at an additional cost of increased transceiver complexity [13], [14]. PD-NOMA has

M.M. Şahin was with the Department of Electrical Engineering, University of South Florida, Tampa, FL, 33620. He is now with Standards and Mobility Innovation Laboratory, Samsung Research America, Plano, TX, 75023, USA (e-mail: m.sahin@samsung.com).

O. Dizdar was with the Imperial College of London, SW7 2AZ London, U.K. He is now with VIAVI Solutions UK Ltd., SG1 2AN Stevenage, U.K. (e-mail: onur.dizdar@viavisolutions.com).

B. Clerckx is with the Department of Electrical and Electronic Engineering, Imperial College London, London, SW7 2AZ, U.K. and with Silicon Austria Labs (SAL), Graz A-8010, Austria (e-mail: b.clerckx@imperial.ac.uk; bruno.clerckx@silicon-austria.com)

H. Arslan is with the Department of Electrical and Electronics Engineering, Istanbul Medipol University, Beykoz, 34810 Istanbul, Turkey (e-mail: huseyinarslan@medipol.edu.tr).

been considered as a study-item in 3GPP in the context of 5G standardization process, however, it is not included in the final 5G releases due to their drawbacks in terms of receiver complexity, weakness in mobility, and its performance being dependent on channel strength disparity between users [15]. Furthermore, the design principle of forcing a user to fully decode the interference from other users limits the advantages of PD-NOMA [16]. To overcome the drawbacks of NOMA, several schemes are proposed, such as, waveform-domain NOMA, which is based on the coexistence of different waveforms dedicated to different applications [17]–[19]. It is shown that waveform-domain NOMA provides significant performance improvement in the power-balanced scenario where conventional PD-NOMA is subject to ambiguity region, resulting in a high performance loss.

Stemming from Han-Koboyashi scheme [20], a recently introduced multiple access scheme named rate-splitting multiple access (RSMA) has been shown to encapsulate and surpass the performance of space-division multiple access (SDMA), NOMA, OMA, and physical layer multicasting in multiple antenna networks in terms of spectral and energy efficiency, latency, and resilience to mixed-critical quality of service [3], [21]. RSMA is a flexible multiple access scheme which provides robust management of interference by partially decoding the interference and partially treating the remaining interference as noise. RSMA splits the user messages into common and private parts, and encodes the common parts into one stream while encoding the private parts into separate streams. The obtained streams are precoded, superposed and transmitted over the wireless channel. Each user first decodes the common stream, then performs SIC, and decode their respective private streams. Each receiver reconstructs its original message from the part of its message embedded in the common stream and its intended private stream.

The conceptual demonstration of RSMA in multi-user (MU) multiple-input single-output (MISO) can be seen in Fig. 1a, where the common stream is applied beamforming to cover both users and k -th private stream is directed towards k -th user. To maximize the achievable sum-rate, the power allocation and precoder design for the common and private streams need to be optimized [22]–[25]. RSMA has been shown to provide unique benefits, such as, enhanced spectral and energy efficiency, multiplexing gain, universality by generalizing conventional OMA, SDMA, NOMA, physical-layer multicasting; flexibility by coping with any interference levels, network loads, services, traffic, user deployments; robustness to inaccurate channel state information (CSI) at both transmitter and receiver ends and resilience to mixed-critical quality of service; reliability under short channel codes and low latency [26]–[30].

Orthogonal frequency division multiplexing (OFDM) waveform has been widely studied and deployed in wireless communication standards such as 4G-LTE, 5G-NR and Wi-Fi owing to its low-complexity implementation and robustness against frequency selective channels [31]. However, ‘sinc’ shaped subcarriers of OFDM makes it vulnerable to ICI from various causes, such as, phase noise, Doppler spread, mismatch in local oscillators of receiver and transmitter. Since ICI

destroys the orthogonality of OFDM subcarriers, it results in saturation in data rate and error floor in BER with increasing system power [32].

A method to combat the affects of ICI is to use flexible OFDM symbol duration and sub-carrier spacing (SCS). Hence, mixed numerologies are employed in 5G to cater for different deployment scenarios and core services [33]. Although this approach is efficient to provide the required flexibility, another capacity-limiting factor, INI, is introduced into the system. Mixed numerologies cause both the loss of orthogonality among subcarriers of different numerologies and the difficulty in achieving symbol alignment in time domain [5].

B. Motivation and Our Contributions

Several works can be found on the analysis of RSMA in multicarrier systems [34]–[38]. A resource allocation algorithm to maximize the sum-rate for RSMA-based multicarrier system is proposed in [34] by performing user matching, subcarrier assignment and power allocation among subcarriers. Similarly, a three step resource allocation scheme is proposed in [35], where power allocation on a single subcarrier, matching between user and subcarrier and power allocation among different subcarriers are solved in steps to maximize the sum-rate. Rate-splitting (RS)-based precoding in the overloaded multicarrier multi-group multicast downlink scenario is studied in [36], where a joint max-min fairness and sum-rate optimization problems are formulated. The practical implementation of the proposed algorithm is verified via link-level simulations in [37] by evaluating the bit-error-rate (BER) performance. An application of RSMA for joint communications and jamming with a multicarrier waveform in MISO-BC is studied in [38]. RS-based precoders are designed to perform simultaneous communications with secondary users and jamming of adversarial users. In abovementioned works, RSMA has been considered to address the problems of various systems employing multicarrier waveforms, the problems of the multicarrier waveform itself and its interaction with the wireless propagation channel, *i.e.*, the determination of SCS to manage ICI under mobility, are not addressed.

In [39], the authors show the advantage of RSMA in the SISO system signalling over the OFDM waveform for the first time. The OFDM-RSMA scheme is proposed to provide robustness against ICI, which allows the interference in the OFDM waveform to be partially decoded and partially treated as noise. In this paper, further performance improvement is provided by leveraging multi-numerology concept into the OFDM-RSMA structure. The proposed multi-numerology OFDM-RSMA introduces extra degree of freedom to cope with the interference that breaks the orthogonality of OFDM subcarriers. Even in SISO system which is not the main attention of prevailing RSMA based studies, the proposed multi-numerology OFDM-RSMA scheme provides the highest achievable sum-rate compared to conventional orthogonal frequency division multiple access (OFDMA) and OFDM-NOMA schemes by keeping fair transmission rates among users at the same time. The main contributions of the paper are as follows:

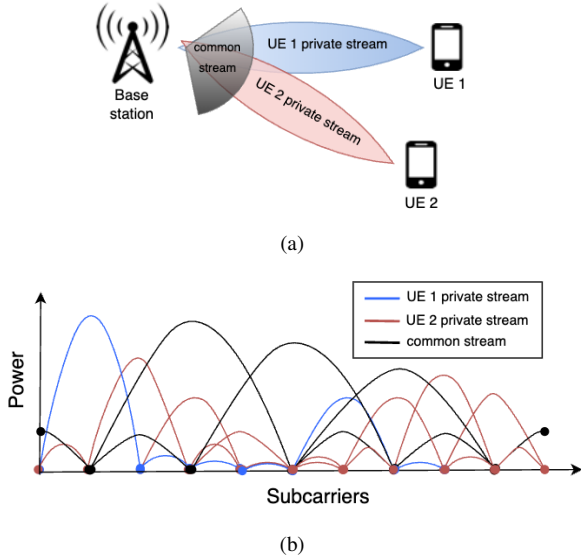


Fig. 1. RSMA schemes in different representations, (a) rate-splitting with multiple antennas at BS, (b) rate-splitting in time-frequency domain using OFDM waveform.

- We construct the analogy between RSMA in MISO-BC and multi-numerology OFDM-RSMA in SISO providing extra degree of freedom to overcome the ICI. Common stream's beam of RSMA in MISO-BC is designed to cover both users allowing interference to be partially decoded and partially treated as noise, whereas beams of private streams are directed to the intended users. For the proposed multi-numerology OFDM-RSMA structure, common stream carrying data of both users also allows interference to be partially decoded and partially treated as noise by having larger SCS than private streams transmitted in the same time-slot. As it can be seen in Fig. 1b private streams are designed to be orthogonal and user specific similar to RSMA in MISO-BC.
- The system model of the OFDM-NOMA is mathematically formulated performing the SIC at the OFDM symbol level rather than the OFDM subcarrier level tackled so far in previous studies [40]–[44]. Aforementioned studies assume that the OFDM-NOMA system is able to both allocate power into subcarriers one by one and change the decoding order at the receiver depending on the power levels of subcarriers which can be fluctuating due to frequency selectivity. In practical wireless systems, the coded-OFDM is commonly implemented where the log-likelihood ratio (LLR) of transmitted bits on subcarriers are calculated and then sent to the decoder in a block manner [33]. This phenomena makes the assumption of subcarrier-dependent decoding order impractical for the OFDM-NOMA architecture, whereas symbol level SIC is performed in this paper to have practical and fair comparison against OFDM-RSMA and OFDMA.
- Rate-augmented weighted minimum mean-square error (AWMMSE) transformations followed by the alternating optimization technique, which is used for RSMA in MISO-BC system [22], are adapted to find the optimal subcarrier and power allocation for the proposed multi-numerology OFDM-RSMA to maximize the sum-rate

under the ICI. The optimization problem is formulated in a way that the proposed scheme is suitable to perform OFDM symbol level transmitter and receiver processing.

- We perform Monte-Carlo simulations to validate the achievable sum-rate gain achieved by the proposed multi-numerology OFDM-RSMA compared to OFDM-NOMA and OFDMA. The impact of different system parameters, such as SCS, and the channel conditions on the performance of OFDM-RSMA are also investigated. We also verify that the proposed multi-numerology OFDM-RSMA reaches more fair rate distribution among users compared to OFDM-NOMA.

The remainder of this paper is organized as follows. Section II describes the utilized channel model and basic OFDM transmission. The proposed OFDM-RSMA method is introduced in Section III. Section IV gives the formulated optimization problem for the OFDM-RSMA framework and the proposed algorithm to solve it. Section V gives the problem formulation for the OFDM-NOMA for comparison. Numerical results are presented in Section VI. The conclusion of the study is drawn in VII.

Notation: Lower-case bold face variables indicate vectors, and upper-case bold face variables indicate matrices. We use \mathbb{C} the set of complex numbers, $\lfloor \cdot \rfloor$ to denote floor operation, \mathbf{I}_N to denote the $N \times N$ identity matrix, $\mathbf{0}$ to denote zero vector with appropriate size, $(\cdot)^T$ to denote transpose, $(\cdot)^*$ to denote complex conjugate, $\Re(\cdot)$ to denote real part of the complex value, $(\cdot)^H$ to denote conjugate transpose, $\mathbb{E}[\cdot]$ to denote expectation. The Euclidean norm, or ℓ_2 -norm, of a vector $x \in \mathbf{R}^n$ is denoted as $\|x\|_2$ and the **Frobenius norm** of a matrix $X \in \mathbf{R}^{m \times n}$ is given by $\|X\|_F$. $\mathbf{A} \odot \mathbf{B}$ and $\mathbf{A} \oslash \mathbf{B}$ correspond to Hadamard multiplication and division of matrices \mathbf{A} and \mathbf{B} ; \mathbf{A}^{o2} denote Hadamard power of matrix \mathbf{A} by two, $\text{diag}(\mathbf{v})$ returns a square diagonal matrix with the elements of vector \mathbf{v} on the main diagonal, $\text{diag}(\mathbf{M})$ returns the elements on the main diagonal of matrix \mathbf{M} in a vector, $\mathcal{CN}(\mu, \sigma^2)$ represents complex Gaussian random vectors with mean μ and variance σ^2 . The notation $(\mathbf{A})_n$ is the n th diagonal element of the matrix \mathbf{A} . Element wise absolute value of vector \mathbf{a} is denoted as $|\mathbf{a}|$, where $|\mathbf{a}| = (|a_0|, \dots, |a_N|)^T$. The notation m_{ij} is the value located in the i th row and the j th column of the matrix \mathbf{M} and \mathbf{e}_i denotes the i th standard unit basis vector of for \mathbb{R}^N .

II. SYSTEM MODEL

We consider the system model with single-antenna transmitter and K single-antenna receivers, indexed by $\mathcal{K} = \{1, 2, \dots, K\}$. In conventional orthogonal transmission, the transmitter performs OFDMA to serve the K users in the allocated time-frequency resource. Channel model and signalling scheme are explained in the following.

A. Channel Model

Throughout the study, time-varying frequency selective fading channels have been used, which are named as doubly dispersive or doubly selective. It produces time and frequency shifts of the transmitted signal due to multipath propagation and Doppler effect. The channel model includes complex

channel gain, Doppler shift and delay for every path. Therefore, the propagation channel in the time-delay domain, $c(t, \tau)$, can be modeled as follows [45]:

$$c(t, \tau) = \sum_{l=1}^L \alpha_l e^{j2\pi\nu_l t} \delta(\tau - \tau_l), \quad (1)$$

where α_l , τ_l , and ν_l denote the complex attenuation factor, time delay, and Doppler frequency shift associated with the l^{th} path where $l \in \{1, 2, \dots, L\}$. Let N and C be the subcarrier number and cyclic prefix (CP) length of the OFDM waveform, respectively. It is assumed that CP length is larger than the maximum delay spread to ensure ISI free transmission. The relation of (1) with the k^{th} user's time domain channel matrix \mathbf{H}_k can be represented as follows:

$$\mathbf{H}_k = \sum_{l=1}^L \alpha_l \mathbf{\Pi}^{n_{\tau_l}} \Delta(\nu_l), \quad (2)$$

where the delay matrix $\mathbf{\Pi}^{n_{\tau_l}} \in \mathbb{C}^{(N+C) \times (N+C)}$ is the forward cyclic shifted permutation matrix according to the delay of the l^{th} path. The delay matrix $\mathbf{\Pi}^{n_{\tau_l}}$ can be expressed as follows:

$$\mathbf{\Pi} = \begin{bmatrix} 0 & 0 & \cdots & 0 & 1 \\ 1 & 0 & \cdots & 0 & 0 \\ 0 & 1 & \cdots & 0 & 0 \\ \vdots & \vdots & \ddots & \vdots & \vdots \\ 0 & 0 & \cdots & 1 & 0 \end{bmatrix}, \quad \text{and} \quad n_{\tau_l} = \left\lfloor \frac{\tau_l}{F_s} \right\rfloor, \quad (3)$$

where F_s is the sampling frequency in the system. The Doppler shift matrix for the l^{th} path, $\Delta(\nu_l) \in \mathbb{C}^{(N+C) \times (N+C)}$, can be written as follows:

$$\Delta(\nu_l) = \text{diag} \left(\left[e^{\frac{j2\pi\nu_l}{F_s}}, e^{\frac{j2\pi\nu_l^2}{F_s}}, \dots, e^{\frac{j2\pi\nu_l(N+C)}{F_s}} \right] \right). \quad (4)$$

Let $\tilde{\mathbf{H}}_k$ be the complete channel frequency response (CFR) matrix of the k^{th} user's channel which is obtained as follows:

$$\tilde{\mathbf{H}}_k = \mathbf{F} \mathbf{B} \mathbf{H}_k \mathbf{A} \mathbf{F}^H, \quad (5)$$

where $\mathbf{F} \in \mathbb{C}^{N \times N}$ is the N -point fast Fourier transform (FFT) matrix, the CP-addition matrix $\mathbf{A} \in \mathbb{N}^{(N+C) \times N}$, and the CP-removal matrix $\mathbf{B}_c \in \mathbb{N}^{N \times (N+C)}$, are defined as follows:

$$\mathbf{A} = \begin{bmatrix} \mathbf{0}_{C \times (N-C)} & \mathbf{I}_C \\ \mathbf{I}_N & \mathbf{0} \end{bmatrix}, \quad \mathbf{B} = \begin{bmatrix} \mathbf{0}_{N \times C} & \mathbf{I}_N \end{bmatrix}.$$

The diagonal components of CFR shown in (5) are the k^{th} user's channel coefficients scaling the subcarrier in interest, shown with a vector $\mathbf{h}_k \in \mathbb{C}^{N \times 1}$ where

$$\mathbf{h}_k = \text{diag}(\tilde{\mathbf{H}}_k), \quad (6)$$

where $k \in \mathcal{K} = \{1, 2, \dots, K\}$. It should be noted that off-diagonal components of CFR represent the ICI due to time variations of the propagation channel.

B. OFDM Transmission for K Users

Throughout the study, it is considered that each user can have different SCS. CP duration of OFDM symbols is C for every user to provide equal robustness against delay spread. Subscript notations are added to FFT, CP addition and removal matrices to differentiate between users. The stream of k^{th} user with the OFDM modulation can be expressed as follows:

$$\mathbf{x}_k = \mathbf{A}_k \mathbf{F}_k^H \text{diag}(\mathbf{p}_k) \mathbf{d}_k, \quad k \in \mathcal{K}, \quad (7)$$

where \mathbf{A}_k , \mathbf{F}_k , \mathbf{p}_k , and \mathbf{d}_k denote CP-addition matrix, FFT matrix, precoding vector, and the communication signal for

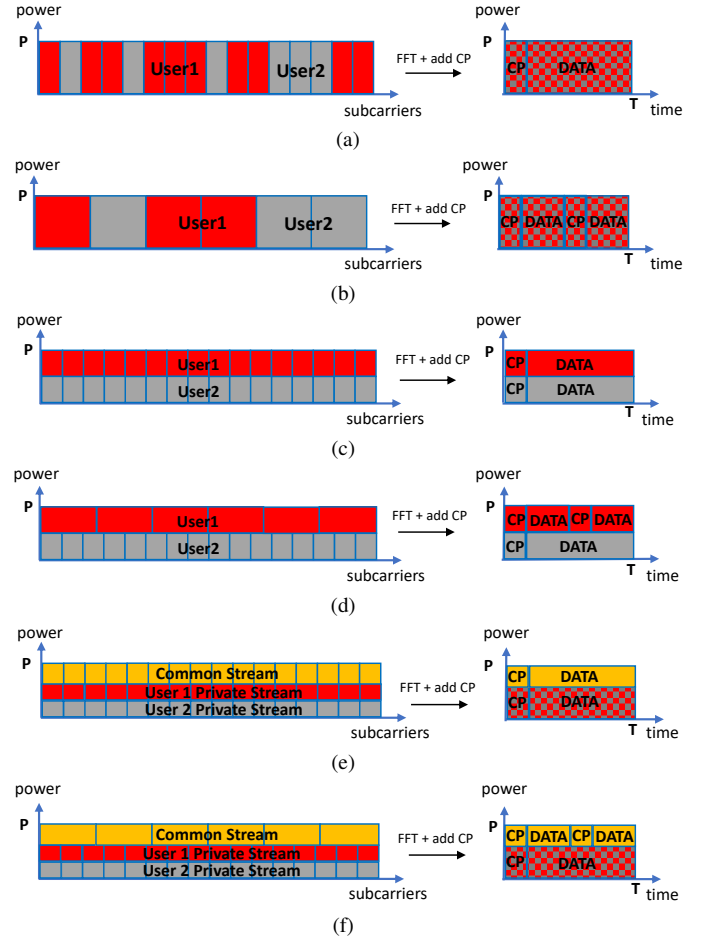


Fig. 2. OFDM based multiple access schemes, (a) OFDMA with narrow SCSs, (b) OFDMA with wide SCSs, (c) OFDM-NOMA with two users having same SCSs, (d) OFDM-NOMA with two users having different SCSs, (e) OFDM-RSMA with two users having same SCS for all three streams, (f) OFDM-RSMA with two users having different SCS between common stream and private streams.

the k^{th} user, respectively. The time-domain received signal, \mathbf{y}_k , after passing through the k^{th} user channel \mathbf{H}_k , can be written as follows:

$$\mathbf{y}_k = \mathbf{H}_k \sum_{k=1}^K \mathbf{x}_k + \mathbf{n}_k. \quad (8)$$

where the vector $\mathbf{n}_k \in \mathbb{C}^{(C+N_p) \times 1}$ is the additive white Gaussian noise (AWGN) with $n_{k_i} \sim \mathcal{CN}(0, \sigma^2)$ where $n_{k_i} \in \mathbf{n}_k$ and σ^2 is the power of AWGN.

III. THE PROPOSED OFDM-RSMA TRANSMISSION SCHEME

In this section, the proposed OFDM-RSMA scheme is introduced where additional data stream modulated via OFDM waveform is integrated into users' dedicated signals utilizing RS based allocation to provide robustness against interference sources, *i.e.*, ICI, INI, and MUI. The message intended for user- k , W_k , is split into common and private parts, which are denoted as $W_{c,k}$ and $W_{p,k}$, $\forall k \in \mathcal{K}$. The common parts of messages for all users are combined into a common message W_c which is encoded into common stream, \mathbf{d}_c . Private part of messages, $W_{p,k}$, are independently encoded into \mathbf{d}_k , $\forall k \in \mathcal{K}$. Fig. 3 demonstrates the proposed RS-based transmission scheme using the OFDM waveform in two users

scenario. The private parts of the split messages of the users are carried on N_p subcarriers with Δf_p SCS. The SCS and number of subcarriers for the combined common message of the users are denoted as Δf_c and N_c , respectively. The subcarrier sets are defined for common and private streams as $\mathcal{N}_c = \{1, \dots, N_c\}$ and $\mathcal{N}_p = \{1, \dots, N_p\}$, respectively. The transmitter uses a cyclic prefix (CP) of length C for private and common streams. For a K -user system, the transmitted private stream $\mathbf{x}_k \in \mathbb{C}^{(C+N_p) \times 1}$ for user- k , and common stream $\mathbf{x}_{c,m} \in \mathbb{C}^{(C+N_p) \times 1}$, are expressed as follows:

$$\mathbf{x}_k = \mathbf{A}_p \mathbf{F}_p^H \text{diag}(\mathbf{p}_k) \mathbf{d}_k, \quad (9a)$$

$$\mathbf{x}_{c,m} = \mathbf{A}_{c,m} \mathbf{F}_c^H \text{diag}(\mathbf{p}_{c,m}) \mathbf{d}_{c,m}, \quad \forall m \in \mathcal{M}, \quad (9b)$$

where the set $\mathcal{M} = \{1, \dots, M\}$ defines the number of common stream's OFDM symbol that can be confined in the duration of private stream with $M = \lfloor \frac{C+N_p}{C+N_c} \rfloor$. The CP-addition matrices for private and common streams, $\mathbf{A}_p \in \mathbb{N}^{(C+N_p) \times N_p}$ and $\mathbf{A}_{c,m} \in \mathbb{N}^{(C+N_p) \times N_c}$, are defined as follows:

$$\mathbf{A}_p = \begin{bmatrix} \mathbf{0}_{C \times (N_p - C)} & \mathbf{I}_C \\ & \mathbf{I}_{N_p} \end{bmatrix}, \mathbf{A}_{c,m} = \begin{bmatrix} \mathbf{0}_{(m-1)(C+N_c)} & & \\ \mathbf{0}_{C \times (N_c - C)} & \mathbf{I}_C & \\ & & \mathbf{I}_{N_c} \\ \mathbf{0}_{(N_p + C - m(N_c + C)) \times N_c} & & \end{bmatrix},$$

where $\mathbf{F}_p \in \mathbb{C}^{N_p \times N_p}$ is the N_p -point FFT matrix, whereas $\mathbf{F}_c \in \mathbb{C}^{N_c \times N_c}$ denotes the N_c -point FFT matrix. The communication signals $\mathbf{d}_k \in \mathbb{C}^{N_p \times 1}$ for k th user private stream, and $\mathbf{d}_{c,m} \in \mathbb{C}^{N_c \times 1}$ for m th common stream are chosen independently from a Gaussian alphabet for theoretical analysis. It is assumed that the streams have unit power, $\mathbb{E}\{\mathbf{d}\mathbf{d}^H\} = \mathbf{I}$, where $\mathbf{d} = [\mathbf{d}_{c,1}^T, \dots, \mathbf{d}_{c,M}^T, \mathbf{d}_1^T, \dots, \mathbf{d}_K^T]^T$. The vectors $\mathbf{p}_k \in \mathbb{C}^{N_p \times 1}$, and $\mathbf{p}_{c,m} \in \mathbb{C}^{N_c \times 1}$ are amplitude values allocated to private and common streams, respectively. The matrix $\mathbf{P} = [\mathbf{p}_1, \dots, \mathbf{p}_K]$ is defined as the collection of all amplitude vectors of private users, $\mathbf{p}_k, \forall k \in \mathcal{K}$. Similarly $\mathbf{P}_c = [\mathbf{p}_{c,1}^T, \dots, \mathbf{p}_{c,M}^T]^T$ corresponds to the collection of all amplitude vectors of common streams, $\mathbf{p}_{c,m}, \forall m \in \mathcal{M}$.

The time-domain received signal, $\mathbf{y}_k \in \mathbb{C}^{(C+N_p) \times 1}$, after passing through the k th user channel $\mathbf{H}_k \in \mathbb{C}^{(C+N_p) \times (C+N_p)}$, can be written as follows:

$$\mathbf{y}_k = \mathbf{H}_k \left(\sum_{m=1}^M \mathbf{x}_{c,m} + \sum_{k=1}^K \mathbf{x}_k \right) + \mathbf{n}_k. \quad (10)$$

At the k th user's receiver, the superimposed signal \mathbf{y}_k is processed with CP removal matrix and FFT operation to convert into frequency domain for equalization and demodulation. Note that the SCS of common stream may be larger than the SCS of common streams from the design perspective, therefore, common and private streams are treated separately. To process the common stream, received signals of users are obtained after passing through the common stream CP removal matrix and FFT matrix whose size is suitable for the length of common stream. The received frequency domain signal at the k th user's m th OFDM symbol, $\mathbf{r}_{c,k,m}$ can be expressed mathematically as follows:

$$\mathbf{r}_{c,k,m} = \mathbf{F}_c \mathbf{B}_{c,m} \mathbf{y}_k, \quad (11)$$

$\mathbf{B}_{c,m} = [\mathbf{0}_{N_c \times (C+(m-1)(C+N_c))}, \mathbf{I}_{N_c}, \mathbf{0}_{N_c \times (C+N_p - m(N_c + C))}]$ is the common stream CP removal matrix. The average received

power at the n th subcarrier ($n \in \mathcal{N}_c$) of $\mathbf{r}_{c,k,m}$ for the certain channel state, $T_{c,k,m,n} \triangleq \mathbb{E}\{|\mathbf{r}_{c,k,m,n}|^2\}$, is written as:

$$T_{c,k,m,n} = \underbrace{\left| s_{n,n}^{c,k,m,n} \right|^2 + \sum_{j=1}^{N_c} \left| \bar{s}_{n,j}^{c,k,m,n} \right|^2 + \sum_{u=1}^K \sum_{j=1}^{N_p} \left| s_{n,j}^{u,m} \right|^2}_{I_{c,k,m,n}} + \sigma^2, \quad (12)$$

where

$$\mathbf{S}^{c,k,m,n} = \mathbf{F}_c \mathbf{B}_{c,m} \mathbf{H}_k \mathbf{A}_{c,m} \mathbf{F}_c^H \text{diag}(p_{c,m,n} \mathbf{e}_n), \quad \forall n \in \mathcal{N}_c,$$

$$\bar{\mathbf{S}}^{c,k,m,n} = \mathbf{F}_c \mathbf{B}_{c,m} \mathbf{H}_k \mathbf{A}_{c,m} \mathbf{F}_c^H \text{diag}(\bar{\mathbf{p}}_{c,m,n}), \quad \forall n \in \mathcal{N}_c,$$

$$\mathbf{S}^{u,m} = \mathbf{F}_c \mathbf{B}_{c,m} \mathbf{H}_k \mathbf{A}_p \mathbf{F}_p^H \text{diag}(\mathbf{p}_u), \quad \forall u \in \mathcal{K},$$

where $\forall k \in \mathcal{K}, \forall m \in \mathcal{M}$ and $\bar{\mathbf{p}}_{c,m,n}$ denotes that n th subcarrier is forced not to carry any energy for the common stream's m th OFDM symbol, i.e., $\bar{\mathbf{p}}_{c,m,n} = [p_{c,m,1}, \dots, p_{c,m,n-1}, 0, p_{c,m,n+1}, \dots, p_{c,m,N_c}]^T$. The k th user's receiver demodulates the common stream, then reconstructs and subtracts from the received signal. With the removal of common stream successfully, FFT matrix succeeding CP removal matrix is applied to the received signal in order to demodulate corresponding private stream as follows:

$$\begin{aligned} \mathbf{r}_k &= \mathbf{F}_p \mathbf{B}_p \left(\mathbf{y}_k - \mathbf{H}_k \sum_{m=1}^M \mathbf{A}_{c,m} \mathbf{F}_c^H \text{diag}(\mathbf{p}_{c,m}) \mathbf{d}_{c,m} \right) \\ &= \mathbf{F}_p \mathbf{B}_p \left(\mathbf{H}_k \sum_{k=1}^K \mathbf{x}_k + \mathbf{n}_k \right), \end{aligned} \quad (13)$$

where $\mathbf{B}_p = [\mathbf{0}_{N_p \times C}, \mathbf{I}_{N_p}]$ is the private stream CP removal matrix. The average received power at the q th subcarrier of \mathbf{r}_k , $T_{k,q} \triangleq \mathbb{E}\{|\mathbf{r}_k|_q|^2\}$, can be written as:

$$T_{k,q} = \underbrace{\left| v_{q,q}^{k,q} \right|^2 + \sum_{j=1}^{N_p} \left| \bar{v}_{q,j}^{k,q} \right|^2 + \sum_{\substack{i=1 \\ i \neq k}}^K \sum_{j=1}^{N_p} \left| w_{q,j}^i \right|^2}_{I_{k,q}} + \sigma^2, \quad (14)$$

where

$$\mathbf{V}^{k,q} = \mathbf{F}_p \mathbf{B}_p \mathbf{H}_k \mathbf{A}_p \mathbf{F}_p^H \text{diag}(p_{k,q} \mathbf{e}_q), \quad \forall k \in \mathcal{K}, \forall q \in \mathcal{N}_p,$$

$$\bar{\mathbf{V}}^{k,q} = \mathbf{F}_p \mathbf{B}_p \mathbf{H}_k \mathbf{A}_p \mathbf{F}_p^H \text{diag}(\bar{\mathbf{p}}_{k,q}), \quad \forall k \in \mathcal{K}, \forall q \in \mathcal{N}_p,$$

$$\mathbf{W}^i = \mathbf{F}_p \mathbf{B}_p \mathbf{H}_k \mathbf{A}_p \mathbf{F}_p^H \text{diag}(\mathbf{p}_i), \quad \forall i \in \mathcal{K} \setminus k,$$

where $\bar{\mathbf{p}}_{k,q}$ denotes that q th subcarrier is forced not to carry any energy for private and common streams, i.e., $\bar{\mathbf{p}}_{k,q} = [p_{k,1}, \dots, p_{k,q-1}, 0, p_{k,q+1}, \dots, p_{k,N_p}]^T$.

By using (12) and (14) SINRs of the common and private streams for a given channel state can be stated as follows:

$$\gamma_{c,k,m,n} \triangleq \left| s_{n,n}^{c,k,m,n} \right|^2 I_{c,k,m,n}^{-1} \quad \text{and} \quad \gamma_{k,q} \triangleq \left| v_{q,q}^{k,q} \right|^2 I_{k,q}^{-1}. \quad (15)$$

The achievable rates for common stream and private streams corresponding to k th user in the corresponding subcarriers can be written as follows:

$$R_{c,k,m,n} = \log_2(1 + \gamma_{c,k,m,n}), \quad R_{k,q} = \log_2(1 + \gamma_{k,q}), \quad (16)$$

and the achievable rates for an OFDM symbol can be written as follows:

$$R_{c,k} = \sum_{m=1}^M \sum_{n=1}^{N_c} R_{c,k,m,n} \text{ bit/s/Hz}, \quad R_k = \sum_{q=1}^{N_p} R_{k,q} \text{ bit/s/Hz}. \quad (17)$$

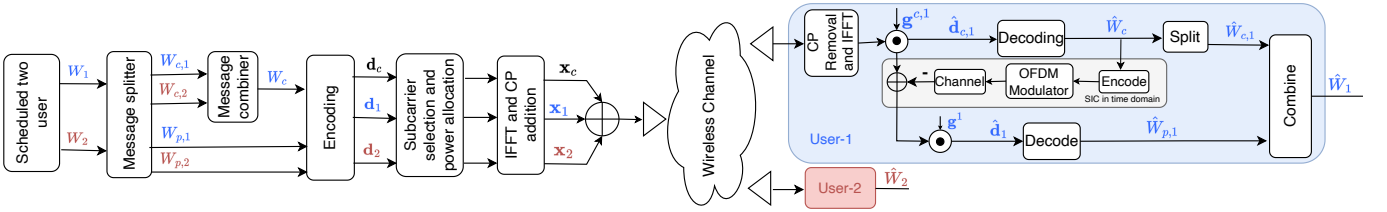


Fig. 3. Proposed OFDM-RSMA transceiver structure.

In the next section, problem formulation to maximize the sum data-rate of the proposed OFDM-RSMA system is provided. Alternation optimization is followed by weighted minimum mean-square error (MMSE) (WMMSE)-based transformation to solve the optimization problem.

IV. PROBLEM FORMULATION AND PROPOSED ALGORITHM FOR OFDM-RSMA

The optimization problem for achievable rate maximization using RSMA with OFDM waveform can be formulated as follows:

$$\begin{aligned} \max_{\mathbf{R}_c, \mathbf{P}_c, \mathbf{P}} \quad & \sum_{m=1}^M \sum_{n=1}^{N_c} R_{c,k,m,n} + \sum_{k=1}^K \sum_{q=1}^{N_p} R_{k,q} \\ \text{s.t.} \quad & \sum_{m=1}^M \sum_{n=1}^{N_c} R_{c,k,m,n} \geq \sum_{m=1}^M \sum_{n=1}^{N_c} R_{c,m,n}, \\ & \|\mathbf{P}\|_F^2 + \|\mathbf{P}_c\|_F^2 \leq P_t, \\ & \sum_{n=1}^{N_c} C_{k,n} + \sum_{q=1}^{N_p} R_{k,q} \geq R_k^{\min}, \forall k \in \mathcal{K}, \end{aligned} \quad (18)$$

where the common rate at the n th subcarrier $R_{c,m,n}$ is shared among users such that $C_{k,m,n}$ is the k th user's portion of the common rate with $R_{c,m,n} = \sum_{k=1}^K C_{k,m,n}$ and \mathbf{R}_c is the collection of $R_{c,k,m,n}, \forall k \in \mathcal{K}, \forall m \in \mathcal{M}, \forall n \in \mathcal{N}_c$.

Let $\hat{\mathbf{d}}_{c,k,m} = \mathbf{g}^{c,k,m} \odot \mathbf{F}_c \mathbf{B}_{c,m} \mathbf{y}_k$ be k th user's estimate of $\mathbf{d}_{c,m}$, where $\mathbf{g}^{c,k,m} \in \mathbb{C}^{N_c \times 1}$ is the one tap-equalizer vector for m th OFDM symbol. After successfully removing the common stream, the estimate of \mathbf{d}_k can be obtained as follows:

$$\hat{\mathbf{d}}_k = \mathbf{g}^k \odot \mathbf{F}_p \mathbf{B}_p \left(\mathbf{y}_k - \mathbf{H}_k \sum_{m=1}^M \mathbf{A}_{c,m} \mathbf{F}_c^H \text{diag}(\mathbf{p}_{c,m}) \hat{\mathbf{d}}_{c,k,m} \right),$$

where \mathbf{g}^k is the corresponding one-tap equalizer vector. At the output of the k th receiver, the common and private mean-squared-errors (MSEs) for n th subcarrier in the m th common stream and q th subcarrier in the private stream are defined as $\varepsilon_{c,k,m,n} \triangleq \mathbb{E} \left\{ \left| \hat{d}_{c,k,m,n} - d_{c,m,n} \right|^2 \right\}$ and $\varepsilon_{k,q} \triangleq \mathbb{E} \left\{ \left| \hat{d}_{k,q} - d_{k,q} \right|^2 \right\}$ respectively, which can be written as follows under the assumptions that common stream has been decoded and removed perfectly:

$$\varepsilon_{c,k,m,n} = \left| g_n^{c,k,m} \right|^2 T_{c,k,m,n} - 2\Re \left\{ g_n^{c,k,m} s_{n,n}^{c,k,m,n} \right\} + 1, \quad (19a)$$

$$\varepsilon_{k,q} = \left| g_q^k \right|^2 T_{k,q} - 2\Re \left\{ g_q^k v_{q,q}^{k,q} \right\} + 1. \quad (19b)$$

Optimum MMSE equalizers for corresponding subcarriers can be found by solving $\frac{\partial \varepsilon_{c,k,m,n}}{\partial g_n^{c,k,m}} = 0$ for $n \in \mathcal{N}_c$, and $\frac{\partial \varepsilon_{k,q}}{\partial g_q^k} = 0$ for $q \in \mathcal{N}_p$,

$$\left(g_n^{c,k,m} \right)^{\text{MMSE}} = T_{c,k,m,n}^{-1} \left(s_{n,n}^{c,k,m,n} \right)^H, \quad (20a)$$

$$\left(g_q^k \right)^{\text{MMSE}} = T_{k,q}^{-1} \left(v_{q,q}^{k,q} \right)^H. \quad (20b)$$

After substituting optimum equalizers found in (20) into equations in (19), MMSEs can be written as follows:

$$\varepsilon_{c,k,m,n}^{\text{MMSE}} \triangleq \min_{g_n^{c,k,m}} \varepsilon_{c,k,m,n} = T_{c,k,m,n}^{-1} I_{c,k,m,n}, \quad (21a)$$

$$\varepsilon_{k,q}^{\text{MMSE}} \triangleq \min_{g_q^k} \varepsilon_{k,q} = T_{k,q}^{-1} I_{k,q}. \quad (21b)$$

From (21), signal-to-interference-plus-noise ratios (SINRs) in (15) and achievable rates in (16) for corresponding subcarriers can be rewritten as follows [46]:

$$\gamma_{c,k,m,n} = \frac{1 - \varepsilon_{c,k,m,n}^{\text{MMSE}}}{\varepsilon_{c,k,m,n}^{\text{MMSE}}}, \quad \text{and} \quad \gamma_{k,q} = \frac{1 - \varepsilon_{k,q}^{\text{MMSE}}}{\varepsilon_{k,q}^{\text{MMSE}}}, \quad (22)$$

$$R_{c,k,m,n} = -\log_2(\varepsilon_{c,k,m,n}^{\text{MMSE}}), \quad R_{k,q} = -\log_2(\varepsilon_{k,q}^{\text{MMSE}}). \quad (23)$$

To solve the optimization problem of (17), the WMMSE method [46] is adapted to the OFDM-RSMA structure. Inspired from [22], the AWMMSE of common and private streams can be written as follows:

$$\zeta_{c,k,m,n} = u_n^{c,k,m} \varepsilon_{c,k,m,n} - \log_2 \left(u_n^{c,k,m} \right), \quad (24a)$$

$$\zeta_{k,q} = u_q^k \varepsilon_{k,q} - \log_2 \left(u_q^k \right), \quad (24b)$$

where $u_n^{c,k,m}, u_q^k > 0$ are weights associated with the k th user's MSEs of common and private stream in the corresponding subcarrier, respectively. To find the rate-AWMMSE relationship, (24) needs to be optimized regarding to equalizers and weights. By solving $\frac{\partial \zeta_{c,k,m,n}}{\partial g_n^{c,k,m}} = 0$ and $\frac{\partial \zeta_{k,q}}{\partial g_q^k} = 0$, the optimum equalizers can be found as $\left(g_n^{c,k,m} \right)^* = \left(g_n^{c,k,m} \right)^{\text{MMSE}}$ and $\left(g_q^k \right)^* = \left(g_q^k \right)^{\text{MMSE}}$.

Substituting these optimum equalizers into (24) yields

$$\zeta_{c,k,m,n} \left(\left(g_n^{c,k,m} \right)^* \right) = u_n^{c,k,m} \varepsilon_{c,k,m,n}^{\text{MMSE}} - \log_2 \left(u_n^{c,k,m} \right), \quad (25a)$$

$$\zeta_{k,q} \left(\left(g_q^k \right)^* \right) = u_q^k \varepsilon_{k,q}^{\text{MMSE}} - \log_2 \left(u_q^k \right). \quad (25b)$$

Then, taking derivative with respect to weight factors and equating to zero as $\frac{\partial \zeta_{c,k,m,n} \left(\left(g_n^{c,k,m} \right)^* \right)}{\partial u_n^{c,k,m}} = 0$ and $\frac{\partial \zeta_{k,q} \left(\left(g_q^k \right)^* \right)}{\partial u_q^k} = 0$, optimum MMSE weights can be obtained as follows:

$$\left(u_n^{c,k,m} \right)^* = \left(u_n^{c,k,m} \right)^{\text{MMSE}} \triangleq \left(\varepsilon_{c,k,m,n}^{\text{MMSE}} \right)^{-1}, \quad (26a)$$

$$\left(u_q^k \right)^* = \left(u_q^k \right)^{\text{MMSE}} \triangleq \left(\varepsilon_{k,q}^{\text{MMSE}} \right)^{-1}, \quad (26b)$$

where the scaling factor of $(\ln(2))^{-1}$ has been omitted without having an impact. By substituting these into (25), the rate-WMMSE relationship is formulated as follows:

Algorithm 1 Alternating Optimization for OFDM-RSMA

- 1: **Initialize:** $n \leftarrow 0$, $\mathbf{P}^{[s]}$, $\mathbf{p}_c^{[s]}$, $\text{SR}^{[s]}$
 - 2: **repeat**
 - 3: $n \leftarrow n + 1$;
 - 4: $\mathbf{P}^{[s-1]} \leftarrow \mathbf{P}^{[s]}$, and $\mathbf{p}_c^{[s-1]} \leftarrow \mathbf{p}_c^{[s]}$;
 - 5: $\mathbf{U} \leftarrow \mathbf{U}^{\text{MMSE}}(\mathbf{P}^{[s-1]}, \mathbf{p}_c^{[s-1]})$;
 - 6: $\mathbf{G} \leftarrow \mathbf{G}^{\text{MMSE}}(\mathbf{P}^{[s-1]}, \mathbf{p}_c^{[s-1]})$;
 - 7: update $(\zeta^c, \mathbf{P}_c, \mathbf{P})$ by solving (28) using the updated \mathbf{U} , and \mathbf{G}
 - 8: **until** convergence in SR is reached
-

$$\zeta_{c,k,m,n}^{\text{MMSE}} \triangleq \min_{u_n^{c,k,m}, g_n^{c,k,m}} \zeta_{c,k,m,n} = 1 - R_{c,k,m,n}, \quad (27a)$$

$$\zeta_{k,q}^{\text{MMSE}} \triangleq \min_{u_q^k, g_q^k} \zeta_{k,q} = 1 - R_{k,q}. \quad (27b)$$

The following sets are defined to denote optimum MMSE equalizers and weights:

$$\mathbf{G}^{\text{MMSE}} \triangleq \left\{ \left(g_n^{c,k,m} \right)^{\text{MMSE}}, \left(g_q^k \right)^{\text{MMSE}} \right\},$$

$$\mathbf{U}^{\text{MMSE}} \triangleq \left\{ \left(u_n^{c,k,m} \right)^{\text{MMSE}}, \left(u_q^k \right)^{\text{MMSE}} \right\},$$

where $k \in \mathcal{K}$, $m \in \mathcal{M}$, $n \in \mathcal{N}_c$, $q \in \mathcal{N}_p$. The deterministic version of AWMSE minimization problem can be formulated as follows:

$$\begin{aligned} & \zeta^c, \mathbf{P}_c, \mathbf{P}, \mathbf{U}, \mathbf{G} \quad \min \quad \sum_{k=1}^K \sum_{m=1}^M \sum_{n=1}^{N_c} \zeta_{c,k,m,n} + \sum_{k=1}^K \sum_{q=1}^{N_p} \zeta_{k,q} \\ & \text{s.t.} \\ & \sum_{m=1}^M \sum_{n=1}^{N_c} \zeta_{c,k,m,n} \leq \sum_{k=1}^K \sum_{m=1}^M \sum_{n=1}^{N_c} X_{c,k,m,n} - MN_c(K-1), \\ & \quad \forall k \in \mathcal{K}, \\ & \|\mathbf{P}\|_F^2 + \|\mathbf{P}_c\|_F^2 \leq P_t, \\ & \sum_{m=1}^M \sum_{n=1}^{N_c} \zeta_{c,k,m,n} + \sum_{q=1}^{N_p} \zeta_{k,q} \leq MN_c + N_p - R_k^{\min}, \end{aligned} \quad (28)$$

where $X_{c,k,m,n} = 1 - C_{c,k,m,n}$ and the transformation of the common rate can be written as follows:

$$\zeta^c = \begin{bmatrix} \zeta_{c,1,1,1} & \cdots & \zeta_{c,1,m,n} & \cdots & \zeta_{c,1,M,N_c} \\ \vdots & \vdots & \ddots & \vdots & \vdots \\ \zeta_{c,k,1,1} & \cdots & \zeta_{c,k,m,n} & \cdots & \zeta_{c,k,M,N_c} \\ \vdots & \vdots & \ddots & \vdots & \vdots \\ \zeta_{c,K,1,1} & \cdots & \zeta_{c,K,m,n} & \cdots & \zeta_{c,K,M,N_c} \end{bmatrix}.$$

It can be seen that solving (28) with respect to \mathbf{U} , and \mathbf{G} leads to MMSE solution of $\mathbf{G}^{\text{MMSE}} \mathbf{U}^{\text{MMSE}}$ formed by corresponding MMSE equalizers and weights. They satisfy the Karush-Kuhn-Tucker (KKT) optimality conditions of (28) for \mathbf{P} and \mathbf{P}_c . For any point $(\zeta^c, \mathbf{P}_c^*, \mathbf{P}^*, \mathbf{U}^*, \mathbf{G}^*)$ satisfying the KKT optimality conditions of (28), the solution satisfies the KKT optimality conditions of (17). Then, the sum-rate problem in (17) is transformed into WMMSE problem of (28). The optimization problem (28) is still non-convex for the joint optimization with respect to parameters. It is shown

that when $(\zeta^c, \mathbf{P}_c, \mathbf{P}, \mathbf{U})$ are fixed, the optimal equalizer is the MMSE equalizer \mathbf{G}^{MMSE} , and when $(\zeta^c, \mathbf{P}_c, \mathbf{P}, \mathbf{G})$ are fixed, the optimal weight is the MMSE weight \mathbf{U}^{MMSE} . When (\mathbf{U}, \mathbf{G}) are fixed, $(\zeta^c, \mathbf{P}_c, \mathbf{P})$ is coupled in the optimization problem (28), closed-form solution cannot be derived. However, it is a convex quadratically constrained quadratic program (QCQP) which can be solved using interior-point methods. These properties lead us to use alternating optimization to solve the problem. In s th iteration of the alternating optimization algorithm, the equalizers and weights are firstly updated using the power allocation matrix obtained in the $(s-1)$ th iteration $(\mathbf{U}, \mathbf{G}) = (\mathbf{U}^{\text{MMSE}}(\mathbf{P}^{[s-1]}, \mathbf{p}_c^{[s-1]}), \mathbf{G}^{\text{MMSE}}(\mathbf{P}^{[s-1]}, \mathbf{p}_c^{[s-1]}))$. $(\zeta^c, \mathbf{P}_c, \mathbf{P})$ can be updated by solving the problem (28), with the updated (\mathbf{U}, \mathbf{G}) . $(\zeta^c, \mathbf{P}_c, \mathbf{P})$ and (\mathbf{U}, \mathbf{G}) are iteratively updated until the sum-rate converges. The details of the alternating optimization algorithm is shown in Algorithm 1, where $\text{SR}^{[s]}$ is the SR calculated based on the updated $(\zeta^c, \mathbf{P}_c, \mathbf{P})$ in s th iteration. The alternating optimization algorithm is guaranteed to converge as sum-rate increasing in each iteration and it is bounded above for a given power constraint. Two steps are followed in every iteration of alternating optimization which are explained below.

1) *Fix the precoder and update equalizers and weights:* The equalizers and weights are updated as $(\mathbf{G}, \mathbf{U}) = (\mathbf{G}^{\text{MMSE}}(\mathbf{P}_c^{[s-1]}, \mathbf{P}^{[s-1]}), \mathbf{U}^{\text{MMSE}}(\mathbf{P}_c^{[s-1]}, \mathbf{P}^{[s-1]}))$ at the s th iteration of the algorithm, where $\mathbf{P}_c^{[s-1]}, \mathbf{P}^{[s-1]}$ are the common and private precoders found at the $(s-1)$ th iteration. The intermediate parameters which are obtained using the updated (\mathbf{G}, \mathbf{U}) can be listed as follows:

$$\begin{aligned} \alpha_{c,k,m} &= \mathbf{u}^{c,k,m} \odot |\mathbf{g}^{c,k,m}|^{\sigma^2}, \\ \alpha_k &= \mathbf{u}^k \odot |\mathbf{g}^k|^{\sigma^2}, \\ \beta_{c,k,m} &= \text{diag} \left((\alpha_{c,k,m})^{\sigma(1/2)} \right) \mathbf{F}_c \mathbf{B}_{c,m} \mathbf{H}_k \mathbf{A}_{c,m} \mathbf{F}_c^H, \\ \beta_{c,p,k,m} &= \text{diag} \left((\alpha_{c,k,m})^{\sigma(1/2)} \right) \mathbf{F}_c \mathbf{B}_{c,m} \mathbf{H}_k \mathbf{A}_p \mathbf{F}_p^H, \\ \beta_k &= \text{diag} \left((\alpha_k)^{\sigma(1/2)} \right) \mathbf{F}_p \mathbf{B}_p \mathbf{H}_k \mathbf{A}_p \mathbf{F}_p^H, \\ f_{c,k,m} &= \text{diag} \left(\mathbf{u}^{c,k,m} \odot \mathbf{g}^{c,k,m} \right) \mathbf{F}_c \mathbf{B}_{c,m} \mathbf{H}_k \mathbf{A}_{c,m} \mathbf{F}_c^H, \\ f_k &= \text{diag} \left(\mathbf{u}^k \odot \mathbf{g}^k \right) \mathbf{F}_p \mathbf{B}_p \mathbf{H}_k \mathbf{A}_p \mathbf{F}_p^H, \\ \mathbf{v}_{c,k,m} &= \log_2 \left(\mathbf{u}^{c,k,m} \right), \quad \text{and} \quad \mathbf{v}_k = \log_2 \left(\mathbf{u}^k \right). \end{aligned}$$

2) *Fix the equalizer and weights update the precoder:* The optimization problem can be written as follows:

$$\begin{aligned} \min_{\zeta^c, \mathbf{P}_c, \mathbf{P}} \quad & \sum_{k=1}^K \left[\sum_{m=1}^M \sum_{n=1}^{N_c} \zeta_{c,k,m,n} + \sum_{q=1}^{N_p} \left(\sum_{\substack{i=1 \\ i \neq k}}^K \sum_{j=1}^{N_p} |\chi_{q,j}^i|^2 + |\kappa_{q,q}^{k,q}|^2 \right. \right. \\ & \left. \left. + \sum_{j=1}^{N_p} |\bar{\kappa}_{q,j}^{k,q}|^2 + (\alpha_k)_q \sigma^2 - 2\Re \{ \omega_q^k \} + u_q^k - v_q^k \right) \right] \end{aligned}$$

s.t.

$$\begin{aligned} & \sum_{m=1}^M \sum_{n=1}^{N_c} \left(\sum_{i=1}^K \sum_{q=1}^{N_p} |\psi_{n,q}^{i,m}|^2 + |\phi_{n,n}^{k,m,n}|^2 + \sum_{j=1}^{N_c} |\bar{\phi}_{n,j}^{k,m,n}|^2 \right. \\ & \left. + (\alpha_{c,k,m})_n + \sigma^2 - 2\Re \{ \omega_n^{c,k} \} \right) \end{aligned}$$

$$\begin{aligned}
& + u_n^{c,k} + v_n^{c,k} \Big) \leq \sum_{k=1}^K \sum_{m=1}^M \sum_{n=1}^{N_c} \zeta_{c,k,m,n}, \\
& \|\mathbf{P}\|_F^2 + \|\mathbf{p}_c\|^2 \leq P_t, \\
& \sum_{m=1}^M \sum_{n=1}^{N_c} \zeta_{c,k,m,n} + \sum_{q=1}^{N_p} \zeta_{k,q} \leq MN_c + N_p - R_k^{\min},
\end{aligned} \tag{29}$$

where

$$\begin{aligned}
\chi^i &= \beta_i \text{diag}(\mathbf{p}_i), \quad \forall i \in \mathcal{K}, \\
\kappa^{k,q} &= \beta_k \text{diag}(\mathbf{p}_{k,q}), \quad \forall k \in \mathcal{K}, \forall q \in N_p, \\
\bar{\kappa}^{k,q} &= \beta_k \text{diag}(\bar{\mathbf{p}}_{k,q}), \quad \forall k \in \mathcal{K}, \forall q \in N_p, \\
\omega^k &= \text{diag}(\mathbf{f}_k \text{diag}(\mathbf{p}_k)), \quad \forall k \in \mathcal{K}, \\
\psi^{i,m} &= \beta_{c,p,i,m} \text{diag}(\mathbf{p}_i), \quad \forall i \in \mathcal{K}, \\
\phi^{k,m,n} &= \beta_{c,k,m} \text{diag}(\mathbf{p}_{c,n}), \quad \forall k \in \mathcal{K}, \forall n \in N_c, \\
\bar{\phi}^{k,m,n} &= \beta_{c,k,m} \text{diag}(\bar{\mathbf{p}}_{c,n}), \quad \forall k \in \mathcal{K}, \forall n \in N_c, \\
\omega^{c,k,m} &= \text{diag}(\mathbf{f}_{c,k,m} \text{diag}(\mathbf{p}_{c,m})), \quad \forall k \in \mathcal{K}.
\end{aligned}$$

In the Section VI, numerical evaluations for the proposed OFDM-RSMA scheme are demonstrated where convex optimization problems are solved using the CVX toolbox [47].

V. OFDM-NOMA TRANSMISSION SCHEME

In the K -user OFDM-NOMA scheme, SIC order for users is not changed throughout one OFDM symbol. Subcarrier-based SIC is not practical since coded-OFDM requires the LLR values across all subcarriers before decoding the user's intended message. The k th user message, \mathbf{x}_k is decoded after $k-1$ users' signal are successively canceled. Unlike the OFDM-RSMA scheme explained in Sec. III, \mathbf{x}_k is designed to convey information of k th user only and there is only one stream dedicated to k th user after removing $k-1$ users' signal. Let the set $\mathcal{M}_k = \{1, \dots, M_k\}$ define the number of OFDM symbol transmitted by k th user in a fixed T duration where $\mathcal{M}_k \in \mathcal{M} = \{\mathcal{M}_1, \dots, \mathcal{M}_K\}$.

At the k th user's receiver, the superimposed signal \mathbf{y}_k is processed with OFDM demodulator after removing all $k-1$ user's signal whose decoding order is earlier than k th user. The received frequency domain signal at the k th user's m th OFDM symbol, $\mathbf{r}_{k,m}$, can be written as follows:

$$\mathbf{r}_{k,m} = \mathbf{F}_k \mathbf{B}_{k,m} \left(\mathbf{y}_k - \mathbf{H}_k \sum_{l=1}^{k-1} \sum_{\eta=1}^{M_l} \mathbf{A}_{l,\eta} \mathbf{F}_l^H \text{diag}(\mathbf{p}_{l,\eta}) \mathbf{d}_{l,\eta} \right) \tag{30}$$

where subscripts k and m are used in order to note that users may utilize different SCS value. For the certain channel state, the average received power, $T_{k,m,q} \triangleq \mathbb{E} \left\{ |(\mathbf{r}_k)_q|^2 \right\}$, at the q th subcarrier of $\mathbf{r}_{k,m}$ can be written as follows:

$$T_{k,m,q} = \underbrace{\left| v_{q,q}^{k,m,q} \right|^2 + \sum_{j=1}^{N_k} \left| \bar{v}_{q,j}^{k,m,q} \right|^2 + \sum_{i=k+1}^K \sum_{j=1}^{N_k} \left| w_{q,j}^{k,i,m} \right|^2}_{I_{k,m,q}} + \sigma^2, \tag{31}$$

where N_k is the total subcarrier number of k th user and

$$\begin{aligned}
\mathbf{V}^{k,m,q} &= \mathbf{F}_k \mathbf{B}_{k,m} \mathbf{H}_k \mathbf{A}_{k,m} \mathbf{F}_k^H \text{diag}(p_{k,m,q} \mathbf{e}_q), \\
\bar{\mathbf{V}}^{k,m,q} &= \mathbf{F}_k \mathbf{B}_{k,m} \mathbf{H}_k \mathbf{A}_{k,m} \mathbf{F}_k^H \text{diag}(\bar{p}_{k,m,q}), \\
\mathbf{W}^{k,i,m} &= \mathbf{F}_k \mathbf{B}_{k,m} \mathbf{H}_k \mathbf{A}_i \mathbf{F}_i^H \text{diag}(\mathbf{p}_i), \quad \forall i \in \{k+1, \dots, K\},
\end{aligned}$$

for the subcarrier set of $\mathcal{N}_k = \{1, 2, \dots, N_k\}$. The vector $\bar{\mathbf{p}}_{k,m,q}$ denotes that q th subcarrier of m th OFDM symbol is forced not to carry any energy, i.e., $\bar{\mathbf{p}}_{k,q} = [p_{k,1}, \dots, p_{k,q-1}, 0, p_{k,q+1}, \dots, p_{k,N_k}]^T$.

The optimization problem for achievable rate maximization using OFDM-NOMA can be formulated as follows:

$$\begin{aligned}
\max_{\mathbf{P}} \quad & \sum_{k=1}^K \sum_{m=1}^{M_k} \sum_{q=1}^{N_k} R_{k,m,q} \\
\text{s.t.} \quad & \|\mathbf{P}\|_F^2 \leq P_t, \\
& R_k \geq R_k^{\min},
\end{aligned} \tag{32}$$

where the matrix $\mathbf{P} = [\mathbf{p}_{1,1}, \dots, \mathbf{p}_{1,M_1}, \dots, \mathbf{p}_{1,M_K}, \dots, \mathbf{p}_{K,M_K}]$ is defined as the collection of all users' precoding vectors, P_t is the total transmit power, and R_k^{\min} is the minimum data rate constraint assigned to k th user. The estimate of m th OFDM symbol of k th user signal in the frequency domain, $\hat{\mathbf{d}}_{k,m}$, can be obtained employing one-tap equalizer vector, $\mathbf{g}^{k,m}$, on $\mathbf{r}_{k,m}$ given in (30). Similar to proposed OFDM-RSMA scheme, rate-AWMMSE transformation can be applied to solve OFDM-NOMA sum-rate optimization problem given in (32).

VI. SIMULATION RESULTS

In this section, the performance of OFDMA, OFDM-NOMA, and OFDM-RSMA is evaluated in a wide variety of channel deployments, such as different channel strengths, Delay and Doppler spread. Several analysis such as achievable rate, fairness, power allocation over different channel conditions in the two-user case are illustrated. Throughout the numerical evaluations, it is assumed that the users and base station (BS) are able to estimate the channel perfectly when they try to design subcarrier and power allocation at the BS and equalizers at the users side. Table I shows the simulation parameters that are used throughout the study. We consider a scenario with $K = 2$, where generalization to more users case can be easily done. Two different SCSs in CP-OFDM waveform is used which are 140 kHz or 60 kHz. Correspondingly, 15 or 35 subcarriers is used in an OFDM symbol whose bandwidth is fixed to 2.1 MHz.

TABLE I
SIMULATION PARAMETERS

Parameter	Value
User Number K	2
SCS	60 kHz or 140 kHz
Subcarrier number	35 or 15
The frame duration	19.04 μ s
CP length in sample	5
CP length duration	2.4 μ s
Sampling rate & Total BW	2.1 MHz
Maximum Delay spread	2 μ s
Maximum Doppler spread	12 kHz

Since the sum-rate optimization problems formed before are non-convex, the initialization of subcarrier and power allocation values, \mathbf{P} and \mathbf{P}_c , is crucial to find the reliable

result. For OFDMA, subcarriers are allocated to users with respect to channel power on corresponding subcarrier. The allocation is done in subcarrier based and orthogonal manner. Besides, power allocation is done with water-filling algorithm after assigning subcarrier to the corresponding user [48]. The similar water-filling procedure is followed to initialize the power and subcarrier allocation for OFDM-NOMA and OFDM-RSMA techniques. It is observed that water-filling based power initialization gives the highest sum-rate among other initialization techniques under the frequency selective channel.

Fig. 2 shows the OFDM based multiple accessing (MA) schemes studied throughout the paper including the conventional OFDMA, OFDM-NOMA, and the proposed OFDM-RSMA. Each scheme serves two users. Multi-numerology OFDM concept is also investigated to make proposed MA schemes more robust in the presence of time selectivity. Fig. 2a and Fig. 2b demonstrate two OFDMA schemes with 60 kHz SCS and 140 kHz SCS, respectively. During an OFDM frame duration T , latter scheme carries two OFDM symbols whereas the former has only one OFDM symbol. Two different OFDM-NOMA configurations are depicted in Fig. 2c and 2d. The SCS of users in the first configuration is same and set as 60 kHz. In the scheme shown in Fig. 2d, the SCS of user-1 is widened to 140 kHz and user-2's SCS remains the same as 60 kHz. It is assumed that the user-1 is the weak user having a smaller overall channel gain than the user-2 (strong user), therefore, user-1 signal is decoded first in the SIC process. Finally, the proposed OFDM-RSMA structure is analyzed with two different configurations that can be seen in Fig. 2e and 2f. Among two configurations, only SCS of common stream changes from 60 kHz to 140 kHz to make the scheme more robust against ICI. The SCS of private streams are determined as 60 kHz.

1) *Achievable Sum-Rate Analysis:* In Fig. 4, the performance of OFDMA, OFDM-NOMA, and OFDM-RSMA are investigated under the frequency selective channel with different Doppler spreads. Here, $\Delta d = \frac{f_d}{\Delta f}$ parameter corresponds to the maximum Doppler spread (f_d) over the subcarrier spacing of 60 kHz ($\Delta f = 60$ kHz). Four cases ($\Delta d = 0$, $\Delta d = 0.1$, $\Delta d = 0.2$, and $\Delta d = 0.4$) are demonstrated in all plots together where $\Delta d = 0$ stands for the frequency selective channel model without any time selectivity.

Fig. 4a demonstrates the performance of three schemes where all streams have 60 kHz SCS in OFDM waveform. For OFDMA, the ICI due to Doppler spread makes the sum-rate curve to saturate for high SNR regime which can be regarded as interference dominated regime. On the other hand, OFDM-NOMA has robustness to ICI because the interference is also decoded and removed when SIC operation is done to remove user-1 signal. Rather, OFDM-RSMA clearly outperforms both OFDMA and OFDM-NOMA in terms of sum-rate gain over all Doppler spread regimes. Utilizing common stream, which introduces data rate to both users, allows us to exploit all power variations of frequency fading channel in OFDM waveform. Also, it provides robustness to ICI mitigation since the interference is partially decoded and partially treated as noise in OFDM-RSMA scheme. With RS, the amount of interference

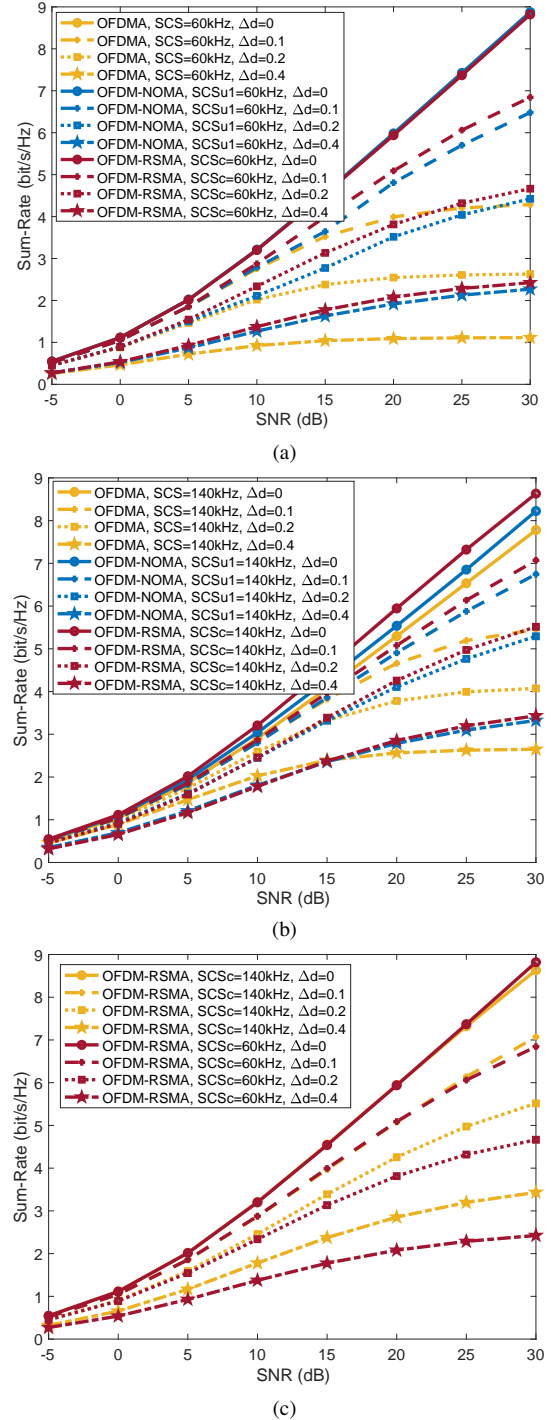


Fig. 4. Sum-rate analysis of proposed OFDM-RSMA scheme compared to conventional OFDMA and OFDM-NOMA under the frequency selective and doubly selective channel (a) SCSs of all streams are set to 60 kHz, (b) SCSs of both users in OFDMA, first user in OFDM-NOMA, and common stream in OFDM-RSMA are set to 140 kHz where user-2 in OFDM-NOMA and private streams in OFDM-RSMA have 60 kHz SCS, (c) different SCSs for common stream in OFDM-RSMA when SCS of private streams is 60 kHz.

decoded by both users (through the presence of common stream) is adjusted dynamically to the channel conditions (channel strength on subcarriers and leakage due to Doppler spread).

Fig. 4b demonstrates the performance of three schemes when both users in OFDMA, user-1 in OFDM-NOMA and common stream in OFDM-RSMA have larger SCS ($\Delta f =$

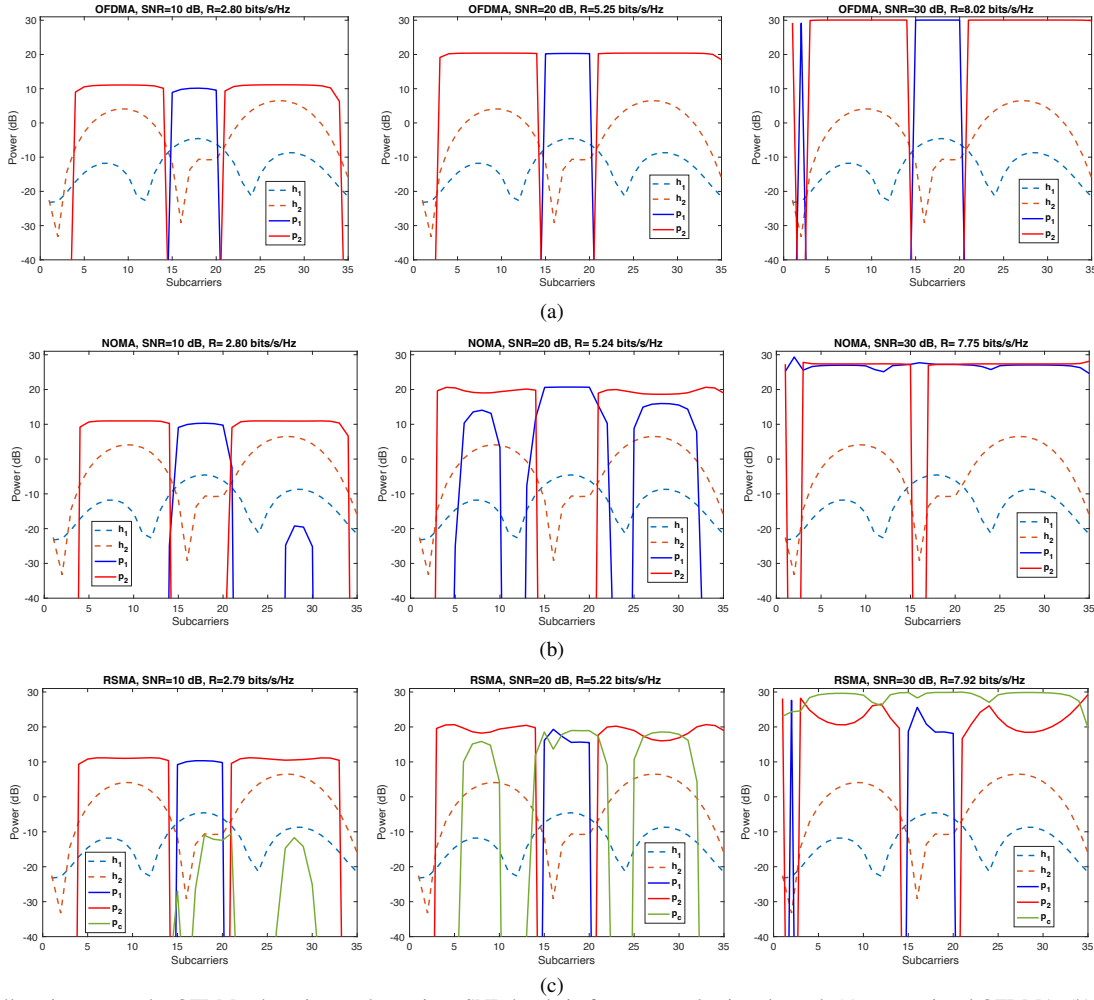


Fig. 5. Power allocation across the OFDM subcarriers under various SNR levels in frequency selective channel, (a) conventional OFDMA, (b) OFDM-NOMA, (c) OFDM-RSMA.

140 kHz); whereas user-2 in OFDM-NOMA and private streams in OFDM-RSMA have narrower SCS ($\Delta f = 60$ kHz). Since the SCS of OFDMA is wider, it can reach higher data rate compared to Fig. 4a under the presence of ICI. However, the sum-rate of OFDMA keeps saturating in high SNR regime. This is because OFDMA does not exploit the interference structure and treats interference as noise. In every regime, OFDM-RSMA outperforms OFDMA and OFDM-NOMA owing to its robust interference management and efficient resource allocation. It can also be seen that additional overhead due to CP lowers sum-rate for OFDMA and OFDM-NOMA when there is no ICI ($\Delta d = 0$).

Fig. 4c shows the effect of different SCS selection in the common stream of OFDM-RSMA on the achievable sum-rate performance. In the no Doppler case with high SNR regime where more power is allocated to common stream, there is a slight decrease in the sum-rate of the scheme with wider SCS in the common stream. It is because of the fact that there are less data subcarriers in the common stream to carry information when its SCS is wider. However, as ICI power increases, the scheme with wider SCS in the common stream outperforms the one with narrower SCS.

2) *Power Allocation Analysis*: Fig. 5 illustrates power allocation of studied MA schemes over the OFDM subcarriers

in the presence of frequency-selective channel without any Doppler spread. Dashed lines show the channel gain of users whereas solid lines are the power levels allocated to corresponding streams. Conventional OFDMA seen in Fig. 5a applies well known waterfilling technique to maximize the sum-rate. The OFDM-NOMA scheme shown in Fig. 5b may prefer orthogonal transmission when one user experiences fading at corresponding subcarrier. Finally, power allocation over subcarriers for the proposed OFDM-RSMA is depicted in Fig. 5c where the power of common stream increases as SNR increases. Also, it can be seen that private streams follow the orthogonal transmission showing that OFDM-RSMA bridges between OFDMA and OFDM-NOMA.

Fig. 6 demonstrates the power allocation analysis in OFDM-NOMA and OFDM-RSMA after the sum-rate maximization problem is solved. Power difference between user-1 and user-2 for OFDM-NOMA can be seen in Fig. 6a whereas power ratio between common and private streams for OFDM-RSMA is shown in Fig. 6b. To gain interference robustness and prevent data loss, OFDM-NOMA allocates more power on user-1 in the interference dominated regime due to ICI. As ICI increases, the more power is allocated to the user-1 stream, as expected. Since the OFDM stream with higher SCS is exposed to less interference under doubly dispersive channel, more

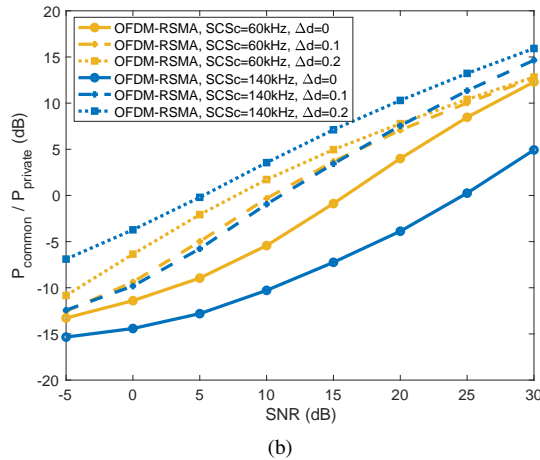
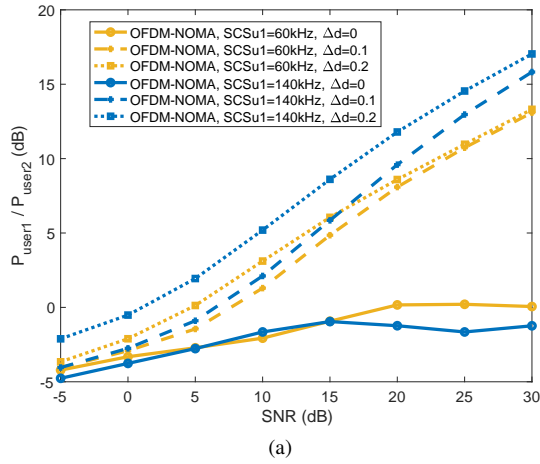


Fig. 6. Power allocation analysis in OFDM-NOMA and OFDM-RSMA schemes, (a) power ratio between user 1 and user 2 in OFDM-NOMA, (b) power ratio between common stream and private streams in OFDM-RSMA.

power is allocated to user-1 when its SCS is at 140 kHz. On the other hand, in OFDM-RSMA scheme, more power is allocated to the common stream to manage the interference as ICI increases which is compatible with MISO BC system under imperfect channel state information at the transmitter (CSIT) scenario [3]. Also, it can be seen that common stream takes less power compared to private streams in noise dominated regime because orthogonal allocation option in private streams provides more flexibility to use frequency selectivity of the channel.

3) *Fairness Analysis*: The fairness analysis of proposed OFDM-RSMA scheme comparing to OFDMA and OFDM-NOMA can be seen in Fig. 7. It illustrates the Jain's fairness index versus SNR in dB. The fairness index, which is in the range of [0, 1] is defined as follows [49]:

$$\frac{\left(\sum_{k=1}^K R_k\right)^2}{K \sum_{k=1}^K R_k^2}.$$

The maximum is achieved in the fairness index when users' rates are equal. Monte Carlo simulation technique is utilized where sum-rates on different channel realization are averaged.

It can be seen that OFDM-NOMA suffers to provide fairness among users for every regimes of ICI because of block decoding property of OFDM causing inefficient use of SIC. In the case of frequency selective channel without any Doppler spread, the fairness index decreases in high SNR

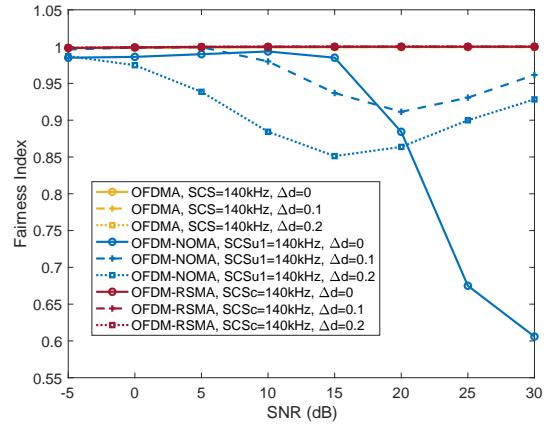


Fig. 7. Fairness comparison of proposed OFDM-RSMA scheme with conventional OFDMA and OFDM-NOMA.

regime because most of the power is allocated to user-2 whose subcarriers can be rescued from being in fading situation after removing the interference of user-1 via SIC. When there is Doppler spread in the channel, more power is allocated to the user-1 whose SCS is large to make the scheme robust against interference. On the other hand, conventional OFDMA and proposed OFDM-RSMA reach the maximum fairness index which is 1 proving that OFDM-RSMA provides fairness among users.

VII. CONCLUSIONS

In this work, we investigate the implementation and validation of RSMA in OFDM waveform under different channel conditions including delay and Doppler spread. Proposed OFDM-RSMA structure is compared with conventional OFDMA and OFDM-NOMA in SISO-BC model. In OFDM-RSMA, common stream decoded by every user are transmitted on top of private streams decoded by the intended user only. Also, OFDM-NOMA scheme is mathematically formulated for the first time, making it suitable for the block-based decoding of OFDM waveform. WMMSE based algorithms are utilized to solve corresponding optimization problems for OFDM-RSMA and OFDM-NOMA techniques. Thanks to its capability for partially decoding interference and partially treating interference as noise, proposed multi-numerology OFDM-RSMA technique provides robustness to ICI where conventional OFDMA is subject to performance limitation due to the loss of orthogonality.

For future study, we will investigate the effect of RSMA along with the OFDM waveform in the multiple antenna systems where combination of errors due to propagation channel such as ICI, ISI and CSIT error is present. Integration of RSMA technique with different waveforms such as orthogonal time-frequency space (OTFS), filter bank multicarrier (FBMC), and single carrier signalling will be studied to find a robust solution against interference due to combination of waveform structure and propagation channel.

REFERENCES

- [1] T. Eichler and R. Ziegler, "Fundamentals of THz technology for 6G by Rohde & Schwarz: White paper:" [Online]. Available: <https://www.rohde-schwarz.com/us/solutions/test-and-measurement/wireless-communication/cellular-standards/6g/white-paper-fundamentals-of-thz-technology-for-6g-by-rohde-schwarz>

- [2] Samsung, "6G the next hyper-connected experience for all," 2021. [Online]. Available: <https://news.samsung.com/global/samsungs-6g-white-paper-lays-out-the-companys-vision-for-the-next-generation-communications-technology>, pp. 12 333–12 337, 2022.
- [3] Y. Mao *et al.*, "Rate-splitting multiple access: Fundamentals, survey, and future research trends," *IEEE Commun. Surveys Tuts.*, pp. 1–1, 2022.
- [4] G. E. Bottomley, *Channel equalization for wireless communications: From concepts to detailed mathematics*. IEEE Press, 2011.
- [5] A. B. Kihero, M. S. J. Solaija, and H. Arslan, "Inter-numerology interference for beyond 5G," *IEEE Access*, vol. 7, pp. 146 512–146 523, 2019.
- [6] A. Huseyin, "OFDM signal analysis and performance evaluation," in *Wireless Communication Signals: A laboratory-based approach*. Wiley, 2021, p. 147–200.
- [7] M. Rebhi *et al.*, "Sparse code multiple access: Potentials and challenges," *IEEE Open J. Commun. Soc.*, vol. 2, pp. 1205–1238, 2021.
- [8] Q. Wang *et al.*, "Non-orthogonal multiple access: A unified perspective," *IEEE Wireless Commun.*, vol. 25, no. 2, pp. 10–16, 2018.
- [9] Y. Chen *et al.*, "Toward the standardization of non-orthogonal multiple access for next generation wireless networks," *IEEE Commun. Mag.*, vol. 56, no. 3, pp. 19–27, 2018.
- [10] H. Lee, S. Kim, and J.-H. Lim, "Multiuser superposition transmission (MUST) for LTE-A systems," in *Proc. IEEE Int. Conf. Commun. (ICC)*, 2016, 2016, pp. 1–6.
- [11] I. Budhiraja *et al.*, "A systematic review on NOMA variants for 5G and beyond," *IEEE Access*, vol. 9, pp. 85 573–85 644, 2021.
- [12] M. Vaezi, H. V. Poor, and Z. Ding, *Multiple access techniques for 5G wireless networks and beyond*. Springer, 2019.
- [13] L. Dai *et al.*, "A survey of non-orthogonal multiple access for 5G," *IEEE Commun. Surveys Tuts.*, vol. 20, no. 3, pp. 2294–2323, 2018.
- [14] S. M. R. Islam *et al.*, "Power-domain non-orthogonal multiple access (NOMA) in 5G systems: Potentials and challenges," *IEEE Commun. Surveys Tuts.*, vol. 19, no. 2, pp. 721–742, 2017.
- [15] B. Makki *et al.*, "A survey of NOMA: Current status and open research challenges," *IEEE Open J. Commun. Soc.*, vol. 1, pp. 179–189, 2020.
- [16] A. Mishra, Y. Mao, O. Dizdar, and B. Clerckx, "Rate-splitting multiple access for 6G - part i: Principles, applications and future works," *IEEE Commun. Lett.*, pp. 1–1, 2022.
- [17] M. M. Şahin and H. Arslan, "Waveform-domain NOMA: The future of multiple access," in *Proc. IEEE Int. Conf. Commun. Workshops (ICC Workshops)*, Jun. 2020, pp. 1–6.
- [18] —, "Application-based coexistence of different waveforms on non-orthogonal multiple access," *IEEE Open J. Commun. Soc.*, vol. 2, pp. 67–79, 2021.
- [19] A. Tusha, S. Doğan, and H. Arslan, "A hybrid downlink NOMA with OFDM and OFDM-IM for beyond 5G wireless networks," *IEEE Signal Process. Lett.*, vol. 27, pp. 491–495, 2020.
- [20] T. Han and K. Kobayashi, "A new achievable rate region for the interference channel," *IEEE Trans. Inf. Theory*, vol. 27, no. 1, pp. 49–60, 1981.
- [21] Y. Mao, B. Clerckx, and V. O. Li, "Rate-splitting multiple access for downlink communication systems: Bridging, generalizing, and outperforming SDMA and NOMA," *EURASIP J. Wireless Commun. Netw.*, vol. 2018, no. 1, 2018.
- [22] H. Joudé and B. Clerckx, "Sum-rate maximization for linearly precoded downlink multiuser MISO systems with partial CSIT: A rate-splitting approach," *IEEE Trans. Commun.*, vol. 64, no. 11, pp. 4847–4861, 2016.
- [23] B. Clerckx, Y. Mao, R. Schober, and H. V. Poor, "Rate-splitting unifying SDMA, OMA, NOMA, and multicasting in MISO broadcast channel: A simple two-user rate analysis," *IEEE Wireless Commun. Lett.*, vol. 9, no. 3, pp. 349–353, 2020.
- [24] B. Matthiesen *et al.*, "Globally optimal spectrum- and energy-efficient beamforming for rate splitting multiple access," *IEEE Trans. Signal Process.*, vol. 70, pp. 5025–5040, 2022.
- [25] A. Mishra, Y. Mao, O. Dizdar, and B. Clerckx, "Rate-splitting multiple access for downlink multiuser MIMO: Precoder optimization and PHY-layer design," *IEEE Trans. Commun.*, vol. 70, no. 2, pp. 874–890, 2022.
- [26] B. Clerckx *et al.*, "A primer on rate-splitting multiple access: Tutorial, myths, and frequently asked questions," *IEEE J. Sel. Areas Commun.*, pp. 1–1, 2023.
- [27] —, "Is NOMA efficient in multi-antenna networks? a critical look at next generation multiple access techniques," *IEEE Open J. Commun. Soc.*, vol. 2, pp. 1310–1343, 2021.
- [28] Y. Mao, B. Clerckx, and V. O. K. Li, "Rate-splitting for multi-antenna non-orthogonal unicast and multicast transmission: Spectral and energy efficiency analysis," *IEEE Trans. Commun.*, vol. 67, no. 12, pp. 8754–8770, 2019.
- [29] Y. Xu *et al.*, "Rate-splitting multiple access with finite blocklength for short-packet and low-latency downlink communications," *IEEE Trans. Commun.*, vol. 70, no. 1, pp. 1–1, 2022.
- [30] R.-J. Reifert, S. Roth, A. Alameer Ahmad, and A. Sezgin, "Comeback Kid: Resilience for Mixed-Critical Wireless Network Resource Management," *arXiv e-prints*, p. arXiv:2204.11878, Apr. 2022.
- [31] Z. E. Ankarali, B. Peköz, and H. Arslan, "Flexible radio access beyond 5G: A future projection on waveform, numerology, and frame design principles," *IEEE Access*, vol. 5, pp. 18 295–18 309, 2017.
- [32] T. Wang, J. Proakis, E. Masry, and J. Zeidler, "Performance degradation of OFDM systems due to Doppler spreading," *IEEE Trans. Wireless Commun.*, vol. 5, no. 6, pp. 1422–1432, 2006.
- [33] E. Dahlman, S. Parkvall, and J. Skold, *5G NR: The Next Generation Wireless Access Technology*, 2nd ed. USA: Academic Press, Inc., 2021.
- [34] J. A. De Castro and F. R. M. Lima, "Subcarrier assignment, user matching and power allocation for weighted sum-rate maximization with RSMA," in *Proc. Global Inf. Infrastruct. Netw. Symp. (GIIS)*, Sep., 2022, pp. 20–24.
- [35] L. Li *et al.*, "Resource allocation for multicarrier rate-splitting multiple access system," *IEEE Access*, vol. 8, pp. 174 222–174 232, 2020.
- [36] H. Chen *et al.*, "Joint power and subcarrier allocation optimization for multigroup multicarrier systems with rate splitting," *IEEE Trans. Veh. Technol.*, vol. 69, no. 2, pp. 2306–2310, 2020.
- [37] —, "Rate-splitting for multicarrier multigroup multicast: Precoder design and error performance," *IEEE Trans. Broadcast.*, vol. 67, no. 3, pp. 619–630, 2021.
- [38] O. Dizdar and B. Clerckx, "Rate-splitting multiple access for communications and jamming in multi-antenna multi-carrier cognitive radio systems," *IEEE Trans. Inf. Forensics Security*, vol. 17, pp. 628–643, 2022.
- [39] M. M. Şahin, O. Dizdar, B. Clerckx, and H. Arslan, "Multicarrier rate-splitting multiple access: Superiority of OFDM-RSMA over OFDMA and OFDM-NOMA," *IEEE Commun. Lett.*, pp. 1–1, 2023.
- [40] T. Kebede, Y. Wondie, J. Steinbrunn, H. B. Kassa, and K. T. Korngay, "Multi-carrier waveforms and multiple access strategies in wireless networks: Performance, applications, and challenges," *IEEE Access*, vol. 10, pp. 21 120–21 140, 2022.
- [41] E. C. Cejudo, H. Zhu, and J. Wang, "Resource allocation in multicarrier NOMA systems based on optimal channel gain ratios," *IEEE Trans. Wireless Commun.*, vol. 21, no. 1, pp. 635–650, 2022.
- [42] J. Zhu, J. Wang, Y. Huang, S. He, X. You, and L. Yang, "On optimal power allocation for downlink non-orthogonal multiple access systems," *IEEE J. Sel. Areas Commun.*, vol. 35, no. 12, pp. 2744–2757, 2017.
- [43] L. Lei *et al.*, "Power and channel allocation for non-orthogonal multiple access in 5G systems: Tractability and computation," *IEEE Trans. Wireless Commun.*, vol. 15, no. 12, pp. 8580–8594, 2016.
- [44] L. Salaün, M. Coupechoux, and C. S. Chen, "Joint subcarrier and power allocation in NOMA: Optimal and approximate algorithms," *IEEE Trans. Signal Process.*, vol. 68, pp. 2215–2230, 2020.
- [45] F. Hlawatsch and G. Matz, *Wireless Communications Over Rapidly Time-Varying Channels*. Elsevier/Academic Press, 2011.
- [46] S. S. Christensen *et al.*, "Weighted sum-rate maximization using weighted MMSE for MIMO-BC beamforming design," *IEEE Trans. Wireless Commun.*, vol. 7, no. 12, pp. 4792–4799, 2008.
- [47] M. Grant and S. Boyd, "CVX: Matlab software for disciplined convex programming, version 2.1," <http://cvxr.com/cvx>, Mar. 2014.
- [48] D. Tse and P. Viswanath, *Fundamentals of Wireless Communication*. USA: Cambridge University Press, 2005.
- [49] A. Salem, C. Masouros, and K.-K. Wong, "Sum rate and fairness analysis for the MU-MIMO downlink under PSK signalling: Interference suppression vs exploitation," *IEEE Trans. Commun.*, vol. 67, no. 9, pp. 6085–6098, 2019.